



HAL
open science

Estimating microbial populations by flow cytometry: Comparison between instruments

Catherine G erikas Ribeiro, Dominique Marie, Adriana Lopes dos Santos,
Frederico Pereira Brandini, Daniel Vaultot

► **To cite this version:**

Catherine G erikas Ribeiro, Dominique Marie, Adriana Lopes dos Santos, Frederico Pereira Brandini, Daniel Vaultot. Estimating microbial populations by flow cytometry: Comparison between instruments. *Limnology and Oceanography: Methods*, 2017, 14 (11), pp.750 - 758. 10.1002/lom3.10135 . hal-01482199

HAL Id: hal-01482199

<https://hal.sorbonne-universite.fr/hal-01482199>

Submitted on 7 Mar 2017

HAL is a multi-disciplinary open access archive for the deposit and dissemination of scientific research documents, whether they are published or not. The documents may come from teaching and research institutions in France or abroad, or from public or private research centers.

L'archive ouverte pluridisciplinaire **HAL**, est destin ee au d ep ot et  a la diffusion de documents scientifiques de niveau recherche, publi es ou non,  emanant des  tablissements d'enseignement et de recherche fran ais ou  trangers, des laboratoires publics ou priv es.

1 **Estimating microbial populations by flow cytometry: comparison between instruments**

2

3 Catherine Gérikas Ribeiro^{1*}, Dominique Marie², Adriana Lopes dos Santos², Frederico Pereira
4 Brandini¹, Daniel Vaultot².

5

6 ¹ Departamento de Oceanografia Biológica, Instituto Oceanográfico, Universidade de São Paulo, São
7 Paulo, Brasil

8 ² Sorbonne Universités, UPMC Univ Paris 06, CNRS, UMR 7144, Station Biologique, Place Georges
9 Teissier, 29680 Roscoff, France

10

11

12 * Corresponding author

13 E-mail: catherine.gerikas@gmail.com (CGR)

14

15 Running head: Estimating microbial populations by FCM

16 Keywords: flow cytometry; microbial oceanography; heterotrophic bacteria; picoplankton;
17 nanoplankton.

18

19 **Abstract**

20 For almost 3 decades, flow cytometry has allowed researchers to investigate ocean planktonic
21 communities using size and cell fluorescence properties. However, oceanographic applications must
22 face two constraints. First, when dealing with marine microbes, instruments must be sensitive because
23 these organisms are very small and with low fluorescence. Second, instruments must be portable to be
24 used on board ships. We compared the performance of two instruments, the BD FACSCanto™ and BD
25 Accuri™ C6. The former is an expensive laboratory-based instrument which has a very good
26 sensitivity, whilst the latter is less sensitive but presents critical advantages for field studies (easy
27 handling and transportation, relatively low cost). We have analyzed 102 samples from the South
28 Atlantic Ocean from 3 transects off Brazil, within the euphotic zone. We compared cell abundance of
29 heterotrophic bacteria, *Prochlorococcus* and *Synechococcus*, as well as photosynthetic pico- and nano-
30 eukaryotes. Heterotrophic bacteria, pico- and nano-eukaryotes could be easily detected with both
31 cytometers. *Prochlorococcus* and *Synechococcus* populations were severely under-estimated with the
32 BD Accuri™ C6, particularly for samples from the well-lit layers of the water column. Correction of
33 abundance data using previously suggested approaches was not sufficient to fully compensate for the
34 low sensibility. Our data suggest that the BD Accuri™ C6 is suitable for counting marine bacteria and
35 photosynthetic eukaryotes, but not *Prochlorococcus* and *Synechococcus*.

36

37

38 **Introduction**

39 Flow cytometry (FCM) is a well-established technique (Marie et al. 1997; Gasol and del
40 Giorgio 2000) used since the 1980s (Trask et al. 1982; Olson et al. 1985) for enumeration and
41 characterization of marine micro-organisms. FCM analysis of planktonic communities fulfills the
42 scientific demands of rapid and accurate cell counting, as it considerably reduces the bias introduced by
43 visual counting (Marie et al. 2005). By simultaneously recording several parameters during analysis,
44 FCM allows the discrimination of pico- and nanoplankton populations and the estimation of their
45 abundance, cell size, and pigment content (Marie et al. 2005), both by natural (chlorophyll,
46 phycoerythrin) or induced (fluorescent dyes) fluorescence (Marie et al. 1997).

47 The flow cytometer registers events as cells are aligned in a fluid stream and flow through a
48 beam of focused light usually provided by one or several lasers. For each particle, scattered light and
49 emitted fluorescence are converted to digital signals and recorded. A flow cytometer comprises three
50 main systems: fluidics (particle transport), optics (laser beam and optical filters), and electronics (signal
51 conversion into electronic data). Detectors for scattered light located at 180° and 90° from the light
52 source are called forward scatter (FSC) and side scatter (SSC), respectively. Fluorescence at different
53 wavelengths (typically green, orange and red) is also recorded. Signals associated with each parameter
54 are displayed as cytograms, which are used to discriminate and count different populations based on
55 scattering and fluorescence features. Phytoplankton populations can be differentiated by FCM
56 according to specific values of the recorded parameters (FSC, SSC, red or orange fluorescence).

57 Bacteria are in general detected after staining with a nucleic acid stain such as SYBR Green-I
58 (Marie et al. 1997). Two different groups can be distinguished based on their apparent nucleic acid
59 content (differences in fluorescence intensity) and side scatter signal (SSC): high nucleic acid (HNA)
60 and low nucleic acid (LNA) bacteria. The function and ecological importance of these two groups is far

61 from being fully understood (Bouvier et al. 2007; Van Wambeke et al. 2011), and several studies have
62 addressed these nucleic acid content differences in terms of ecological traits, such as bacterial activity
63 and production (Morán et al. 2007; Ortega-Retuerta et al. 2008; Van Wambeke et al. 2011).

64 Two main groups of autotrophic prokaryotes dominate picoplankton: *Prochlorococcus* and
65 *Synechococcus*. *Prochlorococcus* is ubiquitous in the euphotic zone of tropical oceans, being
66 considered the most abundant photosynthetic organisms on the planet (Partensky et al. 1999b), and its
67 discovery was only made possible with the development of flow cytometry (Chisholm et al. 1988).
68 *Prochlorococcus* is discriminated by its small scattering and low red fluorescence (chlorophyll).
69 *Synechococcus* is widely distributed in marine environments, being particularly abundant in well-lit
70 and nutrient rich top layers of the oceans (Partensky et al. 1999a). One of the key parameters that
71 allows *Synechococcus* populations to be discriminated by FCM is the phycoerythrin content (orange
72 fluorescence). Different *Synechococcus* clades can show distinct fluorescence signatures (Olson et al.
73 1990; Thompson and van den Engh 2016), as a result of different phycobilisome composition (Scanlan
74 et al. 2009). Pico- and nanoeukaryotes are important contributors to global primary productivity (Li
75 1994), and due to their larger cell size, they often contribute to an important share of autotrophic
76 biomass in the oceans (Zubkov et al. 1998). Picoeukaryotes, which cells range from 0.8 μm to 2-3 μm
77 (Simon et al. 1994), present well-defined cytometric signatures by FCM, while nano-eukaryotes
78 populations are less well defined.

79 FCM analysis has led to numerous advances in marine microbial ecology, although cost and
80 maintenance expenses were prohibitive for many laboratories until recently (Gasol and del Giorgio
81 2000; Vives-Rego et al. 2000). Since the first cytometry-based field study made by Olson, Vaultot &
82 Chisholm (1985), on-board flow cytometry has become a crucial tool in the investigation of both
83 autotrophic and heterotrophic picoplanktonic communities (Legendre et al. 2001). The manufacturing
84 of low cost compact benchtop flow cytometers such as the BD Accuri™ C6, the Millipore Guava® or
85 the Applied Biosystems Attune® has facilitated the use of FCM to study of phytoplankton communities

86 around the world, due to easy handling, automatic sampling and easy transportation (a critical quality
87 for field measurements). However, these low cost instruments can be less sensitive than laboratory
88 based flow cytometers, due to less sophisticated optical and/or electronic systems.

89 A lower sensitivity is usually not a problem for bacteria which are detected after staining with
90 strongly fluorescing dyes such as SYBR Green, or for small eukaryotes whose pigment content is
91 relatively high. However, this is not the case for cyanobacteria like *Prochlorococcus*, for which the
92 concentration of photosynthetic pigments per cell is as much as 50-100 fold lower in cells exposed to
93 high light as a result of photo-acclimation (Sosik et al. 1989; Olson et al. 1990), creating 'dim'
94 populations in the surface layers. Such low fluorescence explains why *Prochlorococcus* escaped
95 detection by researchers using epifluorescence microscopy or even during the first use of FCM on
96 board oceanographic ships (Olson et al. 1985). To overcome the problem of low sensitivity flow
97 cytometers, both direct and indirect approaches to infer *Prochlorococcus* abundance have been
98 developed, such as changes in cytometer optical set up to improve excitation energy or fluorescence
99 detection (Dusenberry and Frankel 1994; Partensky et al. 1999b) and the use of mathematical
100 corrections (Zubkov et al. 1998; Crosbie and Furnas 2001).

101 In this paper, we compare data obtained on marine microbial communities with two flow
102 cytometers, the FACSCanto™ and the Accuri™ C6 (hereafter named as CANTO and C6). Although
103 manufactured by the same company (BD Biosciences, San Jose, CA, USA), these cytometers present
104 distinct fluorescence excitation/detection technical features (Table 1). Differences in laser, optics and
105 electronic systems can potentially affect sensitivity and resolution, influencing the accuracy of field
106 measurements. We analyzed heterotrophic marine bacteria, photosynthetic eukaryotes and
107 cyanobacteria on a set of marine samples from the South Atlantic Ocean (displaying both nutrient and
108 light gradients within the water column). While both instruments produced equivalent data for bacteria
109 and eukaryotes, cyanobacteria, especially *Prochlorococcus*, were severely under-estimated with the C6
110 instrument, and procedures previously suggested to correct the data proved ineffective.

111 **Materials and methods**

112 **Sampling**

113 Water samples were collected onboard the R/V "Alpha Crucis", between 31/10/2013 and
114 23/11/2013. The surveyed area was located between latitude 23°11'S - 30°52'S and longitude 39°22'W
115 - 49°09'W, along 3 transects (TR1, TR2 and TR3), in the South West Atlantic off Brazil, reaching the
116 3510 meters isobath (Fig. 1). The sampling strategy comprised cross-shelf transects with 5 depths per
117 station within the euphotic zone for TR1 and TR2, as well as 12 surface samplings for TR3, for a total
118 of 102 samples. Three water masses were sampled during the cruise: the warm and oligotrophic
119 Tropical Water, the cold and nutrient rich South Atlantic Central Water and the Coastal Water, with
120 highly variable features (Castro et al. 2006). Except for TR3 samples, which were collected using a
121 polycarbonate bucket, seawater samples were collected with 12 L Niskin bottles attached to a Seabird®
122 CTD-rosette system (Sea-Bird Electronics, Bellevue, WA, USA), divided into cryotubes, preserved
123 with 0.1% glutaraldehyde, final concentration (modified from Vaultot et al., 1989), incubated for 10
124 minutes in the dark, flash-frozen in liquid nitrogen and stored at -80°C until analysis.

125 **Flow cytometry analysis**

126 Two flow cytometers were used in this study: a BD FACSCanto II™ and a BD Accuri™ C6
127 (Table 1). Samples were counted simultaneously on both cytometers located in the same room, in order
128 to avoid any possible bias by manipulation or time span between measurements. The tubing of the C6
129 was new and fluidics were calibrated for precise volume measurements as recommended by the
130 manufacturer (Section 4.13 of manual).

131 Samples were first analyzed unstained to enumerate phototrophs. Fluorescent beads (0.95 G
132 Fluoresbrite® Polysciences, Warrington, PA) were added in each sample in order to normalize
133 parameters (Marie et al. 1997). A second analysis was performed to enumerate heterotrophic bacteria

134 after staining with SYBR Green[®] (1:10000, final concentration) (Ref-S7585, Life Technologies,
135 Eugene, Oregon).

136 On the C6, for enumerating phytoplankton, 200 μL of sample were analyzed at the "high" rate
137 ($66 \mu\text{L}\cdot\text{min}^{-1}$) with a threshold set at 700 on red fluorescence (FL3-H). To enumerate heterotrophs, 60
138 μL of SYBR Green stained samples were run at "medium" rate ($35 \mu\text{L}\cdot\text{min}^{-1}$) and the threshold was set
139 at 700 on green fluorescence (FL1-H). In both cases, thresholds were determined by running 0.2 μm
140 filtered sea water sample and lowering the values until electrical or optical noise appears.

141 On the CANTO for enumerating phytoplankton, samples were run for 3 min with a rate of 72
142 $\mu\text{L}\cdot\text{min}^{-1}$ and with the discriminator set on red fluorescence at 200. For bacterial enumeration, SYBR
143 Green stained samples were run for 2 min at a rate of $60 \mu\text{L}\cdot\text{min}^{-1}$ and the threshold was set on green
144 fluorescence at 500. Flow rate was determined by the method described by Marie et al. (1997). A
145 known volume of seawater was injected on the CANTO for at least 10 min. Then the remaining volume
146 is measured and the rate is determined by dividing the difference between initial and final volumes by
147 the injection time.

148 Data were analyzed with the Flowing Software[®] 2.5 (<http://www.flowingsoftware.com>). Each
149 population was identified on the cytograms on the basis of its scatter and fluorescence signals (Fig. S1).
150 Each parameter was normalized to that of the reference beads (0.95 μm). Cell counts for each red
151 fluorescence value were exported from the single parameter histogram. The resulting spreadsheet (File
152 S1) was used in subsequent analysis with the R software (R Development Core Team, 2013).

153 Near the surface the red chlorophyll fluorescence of the picophytoplankton decreases due to
154 photoacclimation (Partensky et al. 1993; Dusenberry et al. 2001; Kulk et al. 2011). Therefore, for a
155 fraction or even all of the *Prochlorococcus* and *Synechococcus* populations, fluorescence can fall
156 below the detection threshold (Fig. 2). For the case where only a part of the population was in the
157 noise, we modified the correction procedure described by Crosbie and Furnas (2001) and implemented
158 it as an R routine (File S2). This correction assumes that the red fluorescence distribution of these

159 populations has a log-normal shape (Crosbie and Furnas 2001; Shapiro 2003) and that, when the left
160 part of the distribution is partially in the noise, the left part can be extrapolated from the right part. The
161 R routine takes as input histograms produced by the Flowing Software[®] (but can be adapted to other
162 data formats) and outputs uncorrected and corrected cell abundance data (output data examples can be
163 found in Files S2 and S3). Three cases can occur for a given population.

- 164 1. The mode of the histogram is not visible (e.g. Fig. 2G). In this case, the population is
165 considered to be mostly within noise, without the possibility of counting or correction. Hence,
166 this population is removed from the dataset and labeled as 'cells in noise' by the R routine.
- 167 2. The mode is visible, but the left part of the distribution is partly below the noise level (e.g. Fig.
168 2A). In this case, the abundance of each population is calculated as the double of the right part
169 of the histogram, from the mode to the maximum, and samples are labeled as 'correction'
- 170 3. The mode is visible and the distribution is totally out of the noise (e.g. Fig. 2C). In this case no
171 correction is performed and the initial output value is kept ('no correction' samples).

172 In some cases, the automatic correction needs some degree of visual confirmation, especially
173 for deeper samples with low cell numbers resulting in noisy histograms (e.g. Fig. 2Q or 2W).
174 Therefore, the R routine provides a graphical output of the histogram for each sample (File S3),
175 allowing the user to visually confirm whether the automatic labeling (case 1, 2, or 3 above) is correct.
176 Statistical analyses were performed with the PRISM[®] 7 software ([http://www.graphpad.com/scientific-](http://www.graphpad.com/scientific-software/prism)
177 [software/prism](http://www.graphpad.com/scientific-software/prism)).

178 **Results**

179 Bacterial populations were well resolved for both CANTO and C6 for all samples (Fig. S1).
180 High Nucleic Acid and Low Nucleic Acid bacterial populations were consistently distinguished with
181 both cytometers and there was a very good correlation for both HNA and LNA ($R^2 = 0.85$ and 0.89 ,
182 respectively) between the data obtained on the different instruments (Fig. 3A, B). For HNA slope was

183 statistically different from 1 ($p < 0.0001$) and abundances estimated by the C6 were consistently lower
184 by 10-15% compared to the CANTO.

185 The chlorophyll fluorescence of *Prochlorococcus* and *Synechococcus* decreases from the deeper
186 layers to the surface in response to photoacclimation. For samples near the surface, cells from both
187 populations can be partly or totally in the noise depending on the instrument sensitivity. Fig. 2
188 demonstrates clearly that the C6 is less sensitive than the CANTO by at least a factor of 10 (note for
189 example Fig. 2C and 2I for *Prochlorococcus* at 110 m for the CANTO and C6, the mode of the
190 histogram is in the noise for the C6 and about 10 times higher than the noise level for the CANTO).
191 With the C6, *Prochlorococcus* populations were completely in the noise above 100 m (55 out of 102
192 samples, Fig. 2 and 4, Table 2) and for *Synechococcus* partly or completely in the noise above 50 m (15
193 out of 102 samples, Fig. 2 and 4, Table 2). With the CANTO, only surface *Prochlorococcus* were
194 partly in the noise and *Synechococcus* was always fully resolved (Fig. 2 and 4, Table 2). When cells
195 were only partly in the noise (i.e. when the histogram mode was clearly visible, e.g. Fig. 2U), we
196 estimated the part of the population that was in the noise using the approach proposed by Crosbie and
197 Furnas (2001) (see Material and Methods section). The comparison between the C6 data which
198 required correction and the CANTO data that did not require correction allowed us to assess the
199 validity of this approach (Fig. 3C and D).

200 Clearly some data points that are corrected (grey squares) appear as outliers and are severely
201 underestimated with the C6, even after correction (Fig. 3C and D). The slopes for non-corrected
202 samples (solid circles) are significantly different from 1 ($p < 0.0001$), being respectively 0.75
203 (*Prochlorococcus*) and 0.77 (*Synechococcus*) (Fig. 3C and D), which corresponds to 25% lower
204 abundance on average with the C6. Vertical cross sections of two transects (Fig. 4) illustrate that, while
205 the CANTO provides fully resolved vertical profiles for both *Prochlorococcus* and *Synechococcus*
206 population, the data from the C6 cannot be used in the upper layer (roughly from 100 m to the surface).

207 Pico- and Nano-eukaryotes were always above the detection limit for both instruments with
208 excellent correlation between the two instruments ($R^2 = 0.94$ and 0.69 , respectively, Fig. 3E and F). As
209 for the other populations, the slopes were significantly different from 1 ($p < 0.0001$). While
210 picoeukaryotes were about 15% more abundant with the C6, it was the reverse for nanoeukaryotes
211 which were slightly underestimated by the C6.

212 Discussion

213 The analysis of planktonic communities by flow cytometry is complex because the distinctive
214 cell features of each population may change with depth, diel cycle and nutrient conditions (e.g. Vaultot
215 and Marie 1999). From the six planktonic groups studied here, four were well resolved by both the
216 CANTO and C6 flow cytometers: HNA and LNA heterotrophic bacteria, autotrophic pico-eukaryotes
217 and nano-eukaryotes. Abundance measured by both instruments were tightly correlated. Abundance
218 was always slightly lower with the C6 than with the CANTO, except for picoeukaryotes. This could
219 have resulted from an imperfect calibration of the analyzed volume for one of the instruments. While
220 on the CANTO, the analyzed volume is manually calibrated, the C6 relies on a calibration every time
221 tubing is changed following the manufacturer's recommendation. However, we have recently observed
222 that the actual volume analyzed varies, even during the course of a day, and needs to be re-calibrated at
223 fixed intervals using a procedure similar to the one used for the CANTO (D. Marie, unpublished data).
224 The slightly lower correlation coefficient observed for nanoeukaryotes could result from the difficulty
225 to clearly distinguish the limits of the pico and nano-eukaryote populations.

226 In contrast, the lower sensitivity of the C6 led a drastic underestimation or even non-detection
227 of the cyanobacteria in the upper 100 m of the water column, especially for *Prochlorococcus*. But the
228 phenomenon was also present for *Synechococcus* although it had not been recognized previously. For
229 both populations, corrections, such as those recommended previously (Zubkov et al. 1998; Crosbie and
230 Furnas 2001), did not completely solve the problem, since in some samples the corrected counts were

231 still much lower than those obtained with the CANTO (Fig. 3C, D). The data obtained with the C6 for
232 *Prochlorococcus* but also *Synechococcus*, should be considered with great caution even when only a
233 part of the population is in the noise.

234 The oceanographic transects (Fig. 4) demonstrate that the C6 instrument would result in very
235 serious underestimates of the cyanobacteria abundance and therefore contribution to the carbon
236 biomass, at least in oligotrophic to mesotrophic waters. For *Synechococcus*, one solution could be to
237 trigger acquisition on PE fluorescence (FL2) which is general quite strong, but this will require to run
238 every sample twice, with the trigger on FL2 and FL3 respectively. Unfortunately this was not tested on
239 our samples. For *Prochlorococcus*, the only solution to overcome the problem of low sensitivity is to
240 increase either the excitation energy or the fluorescence detection through optical solutions
241 (Dusenberry and Frankel 1994; Partensky et al. 1999b).

242 **Conclusion**

243 The increasing affordability of benchtop flow cytometers comes with limitations in some of the
244 equipment features, such as lower detection limits. The comparison between studies of phytoplankton
245 communities by flow cytometry should take into account the equipment used, particularly in
246 approaches involving populations of *Prochlorococcus* and *Synechococcus*, in which low chlorophyll
247 concentration per cell can lead to the underestimation of their abundance in the top euphotic zone. Still
248 these benchtop flow cytometers provide reliable data for other populations such as heterotrophic
249 bacteria and photosynthetic eukaryotes. Our study highlight the need for careful comparison between
250 instruments before using them for large scale oceanographic surveys, using as reference the most
251 sensitive laboratory instruments available.

252

253

254 **Acknowledgments**

255 We thank the officers and crew of the R/V *Alpha Crucis* for logistical support. Financial
256 support for this work was provided by the CNRS Groupement de Recherche International (GDRI)
257 "Diversity, Evolution and Biotechnology of Marine Algae", the COFECUB-CAPES project "Pico
258 Brás" (TE 871-15) and FAPESP - *Fundação de Amparo à Pesquisa do Estado de São Paulo*
259 (2012/04800-9 and 2014/15242-2).

260

261

262 **References**

- 263 Bouvier, T., P. A. del Giorgio, and J. M. Gasol. 2007. A comparative study of the cytometric
264 characteristics of High and Low nucleic-acid bacterioplankton cells from different aquatic
265 ecosystems. *Environ. Microbiol.* **9**: 2050–2066. doi:10.1111/j.1462-2920.2007.01321.x
- 266 Castro, B. M., F. P. Brandini, A. M. S. Pires-Vanin, and L. B. Miranda. 2006. Physical oceanography
267 of the western Atlantic continental shelf located between 4 N and 34 S, p. 209–251. *In* A.R.
268 Robinson and K.H. Brink [eds.], *The Sea, Volume 14A: The Global Coastal Ocean*. Harvard
269 University Press.
- 270 Chisholm, S. W., R. J. Olson, E. R. Zettler, R. Goericke, J. B. Waterbury, and N. A. Welschmeyer.
271 1988. A novel free-living prochlorophyte abundant in the oceanic euphotic zone. *Nature* **334**:
272 340–343. doi:10.1038/334340a0
- 273 Crosbie, N., and M. Furnas. 2001. Abundance, distribution and flow- cytometric characterization of
274 picophytoprokaroyote populations in central (17°S) and southern (20°S shelf waters of the Great
275 Barrier Reef. *J. Plankton Res.* **23**: 809–828. doi:809–828. doi:10.1093/plankt/23.8.809
- 276 Dusenberry, J. A., and S. L. Frankel. 1994. Increasing the sensitivity of a FACScan flow cytometer to
277 study oceanic picoplankton. *Limnol. Oceanogr.* **39**: 206–209. doi:10.4319/lo.1994.39.1.0206
- 278 Dusenberry, J. A., R. J. Olson, and S. W. Chisholm. 2001. Photoacclimation kinetics of single-cell
279 fluorescence in laboratory and field populations of *Prochlorococcus*. *Deep. Res. Part I Oceanogr.*
280 *Res. Pap.* **48**: 1443–1458. doi:10.1016/S0967-0637(00)00096-0
- 281 Gasol, J. M., and P. a del Giorgio. 2000. Using flow cytometry for counting natural planktonic bacteria
282 and understanding the structure of planktonic bacterial communities. *Sci. Mar.* **64**: 197–224.
283 doi:10.3989/scimar.2000.64n2197
- 284 Kulk, G., W. H. van de Poll, R. J. W. Visser, and A. G. J. Buma. 2011. Distinct differences in

- 285 photoacclimation potential between prokaryotic and eukaryotic oceanic phytoplankton. *J. Exp.*
286 *Mar. Bio. Ecol.* **398**: 63–72. doi:10.1016/j.jembe.2010.12.011
- 287 Legendre, L., C. Courties, and M. Troussellier. 2001. Flow cytometry in oceanography 1989-1999:
288 Environmental challenges and research trends. *Cytometry* **44**: 164–172. doi:10.1002/1097-
289 0320(20010701)44:3<164::AID-CYTO1108>3.0.CO;2-6
- 290 Li, W. K. W. 1994. Primary production of prochlorophytes, cyanobacteria, and eucaryotic
291 ultraphytoplankton: Measurements from flow cytometric sorting. *Limnol. Oceanogr.* **39**: 169–175.
292 doi:10.4319/lo.1994.39.1.0169
- 293 Marie, D., F. Partensky, S. Jacquet, and D. Vaultot. 1997. Enumeration and cell cycle analysis of natural
294 populations of marine picoplankton by flow cytometry using the nucleic acid stain SYBR Green I.
295 *Appl. Environ. Microbiol.* **63**: 186–193.
- 296 Marie, D., N. Simon, and D. Vaultot. 2005. Phytoplankton Cell Counting by Flow Cytometry, p. 253–
297 556. *In* R.A. Andersen [ed.], *Algal culturing techniques*. Academic Press.
- 298 Morán, X., A. Bode, L. Suárez, and E. Nogueira. 2007. Assessing the relevance of nucleic acid content
299 as an indicator of marine bacterial activity. *Aquat. Microb. Ecol.* **46**: 141–152.
300 doi:10.3354/ame046141
- 301 Olson, R. J., S. W. Chisholm, and E. R. Zettler. 1990. Pigments, size, and distribution of
302 *Synechococcus* in the North Atlantic and Pacific Oceans. *Limnol. Oceanogr.* **35**: 45–58.
- 303 Olson, R. J., D. Vaultot, and S. W. Chisholm. 1985. Marine phytoplankton distributions measured using
304 shipboard flow cytometry. *Deep Sea Res. Part A. Oceanogr. Res. Pap.* **32**: 1273–1280.
305 doi:10.1016/0198-0149(85)90009-3
- 306 Ortega-Retuerta, E., I. Reche, E. Pulido-Villena, S. Agustí, and C. Duarte. 2008. Exploring the
307 relationship between active bacterioplankton and phytoplankton in the Southern Ocean. *Aquat.*
308 *Microb. Ecol.* **52**: 99–106. doi:10.3354/ame01216
- 309 Partensky, F., J. Blanchot, and D. Vaultot. 1999a. Differential distribution and ecology of

- 310 *Prochlorococcus* and *Synechococcus* in oceanic waters: a review. Bull. l'Institut
311 océanographique.
- 312 Partensky, F., W. R. Hess, and D. Vaolot. 1999b. *Prochlorococcus*, a marine photosynthetic prokaryote
313 of global significance. Microbiol. Mol. Biol. Rev. **63**: 106–127.
- 314 Partensky, F., N. Hoepffner, K. W. O. Ulloa, and D. Vaolot. 1993. Photoacclimation of
315 *Prochlorococcus* sp. (Prochlorophyta) Strains isolated from the northern Atlantic and the
316 Mediterranean sea. Plant Physiol. **101**: 285–296.
- 317 Scanlan, D. J., M. Ostrowski, S. Mazard, and others. 2009. Ecological genomics of marine
318 picocyanobacteria. Microbiol. Mol. Biol. Rev. **73**: 249–299. doi:10.1128/MMBR.00035-08
- 319 Shapiro, H. M. 2003. Practical flow cytometry, 3rd Edition, by Howard M. Shapiro, M.D., Wiley-Liss,
320 Inc., New York, 1995, 542 pages, 4th Ed.
- 321 Simon, N., R. G. Barlow, D. Marie, F. Partensky, D. Vaolot, and Qd. 1994. Characterization of oceanic
322 photosynthetic picoeukaryotes by flow-cytometry. J. Phycol. **30**: 922–935. doi:10.1111/j.0022-
323 3646.1994.00922.x
- 324 Sosik, H. M., S. W. Chisholm, and R. J. Olson. 1989. Chlorophyll fluorescence from single cells:
325 Interpretation of flow cytometric signals. Limnol. Oceanogr. **34**: 1749–1761.
326 doi:10.4319/lo.1989.34.8.1749
- 327 Team R Development Core. 2013. R: A language and environment for statistical computing. R Found.
328 Stat. Comput. 1–3464.
- 329 Thompson, A. W., and G. van den Engh. 2016. A multi-laser flow cytometry method to measure single
330 cell and population-level relative fluorescence action spectra for the targeted study and isolation of
331 phytoplankton in complex assemblages. Limnol. Oceanogr. Methods **14**: 39–49.
332 doi:10.1002/lom3.10068
- 333 Trask, B. J., G. J. van den Engh, and J. H. Elgershuizen. 1982. Analysis of phytoplankton by flow
334 cytometry. Cytometry **2**: 258–264. doi:10.1002/cyto.990020410

- 335 Vault, D., C. Courties, and F. Partensky. 1989. A simple method to preserve oceanic phytoplankton
336 for flow cytometric analyses. *Cytometry* **10**: 629–635. doi:10.1002/cyto.990100519
- 337 Vault, D., and D. Marie. 1999. Diel variability of photosynthetic picoplankton in the equatorial
338 Pacific. *J. Geophys. Res. Ocean.* **104**: 3297–3310. doi:10.1029/98JC01333
- 339 Vives-Rego, J., P. Lebaron, and G. Nebe-von Caron. 2000. Current and future applications of flow
340 cytometry in aquatic microbiology. *FEMS Microbiol. Rev.* **24**: 429–448. doi:10.1111/j.1574-
341 6976.2000.tb00549.x
- 342 Van Wambeke, F., P. Catala, M. Pujo-Pay, and P. Lebaron. 2011. Vertical and longitudinal gradients in
343 HNA-LNA cell abundances and cytometric characteristics in the Mediterranean Sea.
344 *Biogeosciences* **8**: 1853–1863. doi:10.5194/bg-8-1853-2011
- 345 Zubkov, M. V, M. A. Sleigh, G. A. Tarran, P. H. Burkill, and R. J. . Leakey. 1998. Picoplanktonic
346 community structure on an Atlantic transect from 50°N to 50°S. *Deep Sea Res. Part I Oceanogr.*
347 *Res. Pap.* **45**: 1339–1355. doi:10.1016/S0967-0637(98)00015-6
- 348
- 349

350

351 **Tables**

352 **Table 1.** Technical features of BD FACSCanto™ and BD Accuri™ C6 flow cytometers according to
 353 the manufacturer.

Features	BD FACSCanto™	BD Accuri™ C6
Weight	149.7 kg	13.6 kg
Acquisition Software	BD FACSDiva	BD CSampler™
Signal Processing	Digital	Digital
Number of lasers	2	2
Total PMT^(a) for fluorescence	8	4
Laser configuration	Blue/red	Blue/red
Laser wavelength	488 nm, 20 mW solid state 633 nm, 17 mW HeNe	488nm; 50mW solid state 640nm; 30mW diode
Excitation light	Optic fiber	Direct
Fluorescence sensitivity	FITC ^(b) < 100 MESF ^(c) PE ^(d) < 50 MESF	FITC < 150 MESF PE < 100 MESF
Optical alignment	Fixed alignment	Fixed alignment
Fluidics	Positive-pressure pump	Peristaltic pump
Sample acquisition	18 bits / 5 decades	24 bits / 7 decades
Sample processing	Tubes	Tubes/96-well plates

354 a) PMT: photomultiplier; b) FITC: fluorescein isothiocyanate; c) MESF: molecules of equivalent
 355 soluble fluorochrome; d) PE: phycoerythrin.

356

357

358 **Table 2.** Number of samples assigned as 'correction', 'no correction' and 'cells in noise' for each pico-
359 cyanobacteria group and equipment tested.

	No correction	Correction	Cells in noise
CANTO - <i>Prochlorococcus</i>	74	27	1
C6 - <i>Prochlorococcus</i>	27	20	55
CANTO - <i>Synechococcus</i>	101	1	0
C6 - <i>Synechococcus</i>	58	29	15

360

361

362

363 **Figure legends**

364 **Fig. 1.** Stations sampled in the South Atlantic Ocean off Brazil during the CARBOM cruise in 2013.
 365 Profiles: transect 1 (TR1, shaded circles) ; transect 2 (TR2, shaded triangles) and surface sampling,
 366 transect 3 (TR3, shaded squares). The grey scale on the right indicates bottom depths.

367

368 **Figure 2.** Examples of depth profiles (St. 100 and St. 114) of normalized red fluorescence distribution
 369 (relative cell number *versus* chlorophyll fluorescence) and cell abundance for *Prochlorococcus* (**a-l**)
 370 and *Synechococcus* (**m-x**) on BD FACSCanto™ and BD Accuri™ C6. For each distribution, it is
 371 indicated whether the cells were in the noise (Noise) or whether a correction was needed (Corr.). In the
 372 depth profiles (**f, l, r, x**), solid symbols represent samples for which no correction was needed; grey
 373 symbols indicate samples for which we applied a correction (see Materials and Methods); samples
 374 within noise were removed.

375

376 **Figure 3.** Relationship between abundance measurements performed with BD Accuri™ C6 and BD
 377 FACSCanto™ (in cells.mL⁻¹): (**a**) HNA bacteria; (**b**) LNA bacteria; (**c**) *Prochlorococcus*; (**d**)
 378 *Synechococcus*; (**e**) picoeukaryotes and (**f**) nanoeukaryotes. For *Prochlorococcus* and *Synechococcus*:
 379 'no correction': solid circles, 'correction': grey squares; 'cells in noise': open triangles. The coefficient of
 380 determination and the equation are indicated on each graphic. The regression line calculated from 'no
 381 correction' samples is marked in black. All the slopes differed significantly from 1 ($p < 0.0001$), except
 382 for LNA bacteria ($p = 0.049$).

383

384 **Figure 4.** Vertical abundance distribution (cells.mL⁻¹) for measurements with BD FACSCanto™ (left
 385 column) and BD Accuri™ C6 (right column): *Prochlorococcus* (**a, b, e, f**) and *Synechococcus* (**c, d, g,**
 386 **h**). Top labels correspond to station number. Sampled points are marked as: 'no correction' (solid
 387 circles), 'correction' (grey squares), or 'cells in noise' (open triangles). Figures were drawn with the
 388 Ocean Data View software (<https://odv.awi.de/>).

389

390

391 Supplementary material is available at <https://figshare.com/s/a9499d9ab4f4740eb576> .

392 **Supplementary figure legend**

393 **Figure S1.** Cytograms of phycoerythrin *versus* chlorophyll fluorescence (**a, b**), side scatter *versus*
394 chlorophyll fluorescence (**c, d**) and side scatter *versus* DNA fluorescence (**e, f**) for sample 137 (St. 100,
395 110 meters depth) for BD FACSCanto™ and BD Accuri™ C6 analyses, showing the gating windows:
396 *Prochlorococcus* (pink), *Synechococcus* (green), picoeukaryotes (blue) nanoeukaryotes (orange), HNA
397 bacteria (yellow) and LNA bacteria (red). Calibrations beads are marked in black.

398

400 **Supplementary material**401 **File S1.** Example of input file for R routine.

channel	sample135_C6_PRO_5m	sample136_C6_PRO_50m	sample137_C6_PRO_110m	sample138_C6_PRO_130m	sample139_C6_PRO_170m
1	0	0	0	0	0
2	0	0	0	0	0
3	0	0	0	0	0
4	0	0	0	0	0
5	0	0	0	0	0
6	0	0	0	0	0
7	0	0	0	0	0
8	0	0	0	0	0
9	0	0	0	0	0
10	0	0	0	0	0
11	0	0	0	0	0
12	0	0	0	0	0
13	0	0	0	0	0
14	0	0	0	0	0
15	0	0	0	0	0
16	0	0	0	0	0
17	0	0	0	0	0
18	0	0	0	0	0
19	0	0	0	0	0
20	0	0	0	0	0
21	0	0	0	0	0
22	0	0	0	0	0
23	0	0	0	0	0
24	0	0	0	0	0
25	0	0	0	0	0
26	0	0	0	0	0
27	0	0	0	0	0
28	0	0	0	0	0
29	0	0	0	0	0
30	0	0	0	0	0
31	0	0	0	0	0
32	0	0	0	0	0
33	0	0	0	0	0
34	0	0	0	0	0
35	0	0	0	0	0

36	0	0	0	0	0
37	0	0	0	0	0
38	0	0	0	0	0
39	0	0	0	0	0
40	0	0	0	0	0
41	0	0	0	0	0
42	0	0	0	0	0
43	0	0	0	0	0
44	0	0	0	0	0
45	0	0	0	0	0
46	0	0	0	0	0
47	0	0	0	0	0
48	0	0	0	0	0
49	0	0	0	0	0
50	0	0	0	0	0
51	0	0	0	0	0
52	0	0	0	0	0
53	0	0	0	0	0
54	0	0	0	0	0
55	0	0	0	0	0
56	0	0	0	0	0
57	0	0	0	0	0
58	0	0	0	0	0
59	0	0	0	0	0
60	0	0	0	0	0
61	0	0	0	0	0
62	0	0	0	0	0
63	0	0	0	0	0
64	0	0	0	0	0
65	0	0	0	0	0
66	0	0	0	0	0
67	0	0	0	0	0
68	0	0	0	0	0
69	0	0	0	0	0
70	0	0	0	0	0
71	0	0	0	0	0
72	0	0	0	0	0
73	0	0	0	0	0
74	0	0	0	0	0
75	0	0	0	0	0
76	0	0	0	0	0
77	0	0	0	0	0
78	0	0	0	0	0

79	0	0	0	0	0
80	0	0	0	0	0
81	0	0	0	0	0
82	0	0	0	0	0
83	0	0	0	0	0
84	0	0	0	0	0
85	0	0	0	0	0
86	0	0	0	0	0
87	0	0	0	0	0
88	0	0	0	0	0
89	0	0	0	0	0
90	0	0	0	0	0
91	0	0	0	0	0
92	0	0	0	0	0
93	0	0	0	0	0
94	0	0	0	0	0
95	0	0	0	0	0
96	0	0	0	0	0
97	0	0	0	0	0
98	0	0	0	0	0
99	0	0	0	0	0
100	0	0	0	0	0
101	0	0	0	0	0
102	0	0	0	0	0
103	0	0	0	0	0
104	0	0	0	0	0
105	0	0	0	0	0
106	0	0	0	0	0
107	0	0	0	0	0
108	0	0	0	0	0
109	0	0	0	0	0
110	0	0	0	0	0
111	0	0	0	0	0
112	0	0	0	0	0
113	0	0	0	0	0
114	0	0	0	0	0
115	0	0	0	0	0
116	0	0	0	0	0
117	0	0	0	0	0
118	0	0	0	0	0
119	0	0	0	0	0
120	0	0	0	0	0
121	0	0	0	0	0

122	0	0	0	0	0
123	0	0	0	0	0
124	0	0	0	0	0
125	0	0	0	0	0
126	0	0	0	0	0
127	0	0	0	0	0
128	0	0	0	0	0
129	0	0	0	0	0
130	0	0	0	0	0
131	0	0	0	0	0
132	0	0	0	0	0
133	0	0	0	0	0
134	0	0	0	0	0
135	0	0	0	0	0
136	0	0	0	0	0
137	0	0	0	0	0
138	0	0	0	0	0
139	0	0	0	0	0
140	0	0	0	0	0
141	0	0	0	0	0
142	0	0	0	0	0
143	0	0	0	0	0
144	0	0	0	0	0
145	0	0	0	0	0
146	0	0	0	0	0
147	0	0	0	0	0
148	0	0	0	0	0
149	0	0	0	0	0
150	0	0	0	0	0
151	0	0	0	0	0
152	0	0	0	0	0
153	0	0	0	0	0
154	0	0	0	0	0
155	0	0	0	0	0
156	0	0	0	0	0
157	0	0	0	0	0
158	0	0	0	0	0
159	0	0	0	0	0
160	0	0	0	0	0
161	0	0	0	0	0
162	0	0	0	0	0
163	0	0	0	0	0
164	0	0	0	0	0

165	0	0	0	0	0
166	0	0	0	0	0
167	0	0	0	0	0
168	0	0	0	0	0
169	0	0	0	0	0
170	0	0	0	0	0
171	0	0	0	0	0
172	0	0	0	0	0
173	0	0	0	0	0
174	0	0	0	0	0
175	0	0	0	0	0
176	0	0	0	0	0
177	0	0	0	0	0
178	0	0	0	0	0
179	0	0	0	0	0
180	0	0	0	0	0
181	0	0	0	0	0
182	0	0	0	0	0
183	0	0	0	0	0
184	0	0	0	0	0
185	0	0	0	0	0
186	0	0	0	0	0
187	0	0	0	0	0
188	0	0	0	0	0
189	0	0	0	0	0
190	0	0	0	0	0
191	0	0	0	0	0
192	0	0	0	0	0
193	0	0	0	0	0
194	0	0	0	0	0
195	0	0	0	0	0
196	442	440	303	0	0
197	1104	1055	963	0	0
198	1647	1615	1519	9	0
199	1664	1604	1696	203	0
200	1385	1362	1440	545	0
201	1158	1123	1241	851	0
202	933	939	1048	882	0
203	748	760	898	716	0
204	590	591	745	543	0
205	479	474	661	421	0
206	376	362	566	322	0
207	286	283	529	239	0

208	203	198	494	184	0
209	147	149	488	135	0
210	103	102	478	100	0
211	80	77	463	71	0
212	56	56	475	53	0
213	43	41	486	36	0
214	35	30	491	22	0
215	24	21	489	16	0
216	16	12	492	13	1
217	10	7	488	12	6
218	9	5	501	12	9
219	7	5	491	9	11
220	6	6	509	7	10
221	3	5	507	6	10
222	2	4	511	7	9
223	2	3	491	7	8
224	3	3	472	5	8
225	2	3	450	5	9
226	2	2	435	5	8
227	1	1	408	8	9
228	0	0	384	9	8
229	0	0	357	11	9
230	1	0	343	10	7
231	2	1	330	11	8
232	2	1	302	11	8
233	1	1	271	14	8
234	1	0	237	16	6
235	1	1	224	18	6
236	1	0	205	17	6
237	0	0	190	20	7
238	1	0	180	22	7
239	1	0	175	31	7
240	1	0	166	34	7
241	0	0	160	35	8
242	0	0	156	43	11
243	0	0	157	48	14
244	0	0	149	58	16
245	0	0	140	59	20
246	0	0	143	66	22
247	0	0	148	71	24
248	0	0	148	84	25
249	0	0	142	91	33
250	0	0	134	94	40

251	0	0	136	101	46
252	0	0	131	112	48
253	0	0	124	126	54
254	0	0	112	130	56
255	0	0	107	126	67
256	0	0	107	127	68
257	0	0	106	127	77
258	0	0	97	125	75
259	0	0	85	121	74
260	0	0	68	114	75
261	0	0	56	120	73
262	0	0	51	117	79
263	0	0	48	123	75
264	0	0	46	108	73
265	0	0	39	107	71
266	0	0	34	93	68
267	0	0	27	89	64
268	0	0	19	75	61
269	0	0	13	73	60
270	0	0	10	73	59
271	0	0	11	65	55
272	0	0	10	56	48
273	0	0	8	43	43
274	0	0	6	39	36
275	0	0	5	35	36
276	0	0	3	27	32
277	0	0	3	26	28
278	0	0	3	18	22
279	0	0	3	17	18
280	0	0	3	13	20
281	0	0	2	11	18
282	0	0	3	9	18
283	0	0	3	6	13
284	0	0	4	5	10
285	0	0	3	5	7
286	0	0	2	5	9
287	0	0	2	5	10
288	0	0	1	3	12
289	0	0	2	2	8
290	0	0	1	2	6
291	0	0	1	3	4
292	0	0	1	3	4
293	0	0	0	2	3

294	0	0	0	1	2
295	0	0	0	1	1
296	0	0	0	1	2
297	0	0	0	1	2
298	0	0	0	0	1
299	0	0	0	0	2
300	0	0	0	0	3
301	0	0	0	0	3
302	0	0	0	0	2
303	0	0	0	0	1
304	0	0	0	0	1
305	0	0	0	0	2
306	0	0	0	0	1
307	0	0	0	0	0
308	0	0	0	0	0
309	0	0	0	0	0
310	0	0	0	0	0
311	0	0	0	0	0
312	0	0	0	0	0
313	0	0	0	0	0
314	0	0	0	0	0
315	0	0	0	0	0
316	0	0	0	0	0
317	0	0	0	0	0
318	0	0	0	0	0
319	0	0	0	0	0
320	0	0	0	0	0
321	0	0	0	0	0
322	0	0	0	0	0
323	0	0	0	0	0
324	0	0	0	0	0
325	0	0	0	0	0
326	0	0	0	0	0
327	0	0	0	0	0
328	0	0	0	0	0
329	0	0	0	0	0
330	0	0	0	0	0
331	0	0	0	0	0
332	0	0	0	0	0
333	0	0	0	0	0
334	0	0	0	0	0
335	0	0	0	0	0
336	0	0	0	0	0

337	0	0	0	0	0
338	0	0	0	0	0
339	0	0	0	0	0
340	0	0	0	0	0
341	0	0	0	0	0
342	0	0	0	0	0
343	0	0	0	0	0
344	0	0	0	0	0
345	0	0	0	0	0
346	0	0	0	0	0
347	0	0	0	0	0
348	0	0	0	0	0
349	0	0	0	0	0
350	0	0	0	0	0
351	0	0	0	0	0
352	0	0	0	0	0
353	0	0	0	0	0
354	0	0	0	0	0
355	0	0	0	0	0
356	0	0	0	0	0
357	0	0	0	0	0
358	0	0	0	0	0
359	0	0	0	0	0
360	0	0	0	0	0
361	0	0	0	0	0
362	0	0	0	0	0
363	0	0	0	0	0
364	0	0	0	0	0
365	0	0	0	0	0
366	0	0	0	0	0
367	0	0	0	0	0
368	0	0	0	0	0
369	0	0	0	0	0
370	0	0	0	0	0
371	0	0	0	0	0
372	0	0	0	0	0
373	0	0	0	0	0
374	0	0	0	0	0
375	0	0	0	0	0
376	0	0	0	0	0
377	0	0	0	0	0
378	0	0	0	0	0
379	0	0	0	0	0

380	0	0	0	0	0
381	0	0	0	0	0
382	0	0	0	0	0
383	0	0	0	0	0
384	0	0	0	0	0
385	0	0	0	0	0
386	0	0	0	0	0
387	0	0	0	0	0
388	0	0	0	0	0
389	0	0	0	0	0
390	0	0	0	0	0
391	0	0	0	0	0
392	0	0	0	0	0
393	0	0	0	0	0
394	0	0	0	0	0
395	0	0	0	0	0
396	0	0	0	0	0
397	0	0	0	0	0
398	0	0	0	0	0
399	0	0	0	0	0
400	0	0	0	0	0
401	0	0	0	0	0
402	0	0	0	0	0
403	0	0	0	0	0
404	0	0	0	0	0
405	0	0	0	0	0
406	0	0	0	0	0
407	0	0	0	0	0
408	0	0	0	0	0
409	0	0	0	0	0
410	0	0	0	0	0
411	0	0	0	0	0
412	0	0	0	0	0
413	0	0	0	0	0
414	0	0	0	0	0
415	0	0	0	0	0
416	0	0	0	0	0
417	0	0	0	0	0
418	0	0	0	0	0
419	0	0	0	0	0
420	0	0	0	0	0
421	0	0	0	0	0
422	0	0	0	0	0

423	0	0	0	0	0
424	0	0	0	0	0
425	0	0	0	0	0
426	0	0	0	0	0
427	0	0	0	0	0
428	0	0	0	0	0
429	0	0	0	0	0
430	0	0	0	0	0
431	0	0	0	0	0
432	0	0	0	0	0
433	0	0	0	0	0
434	0	0	0	0	0
435	0	0	0	0	0
436	0	0	0	0	0
437	0	0	0	0	0
438	0	0	0	0	0
439	0	0	0	0	0
440	0	0	0	0	0
441	0	0	0	0	0
442	0	0	0	0	0
443	0	0	0	0	0
444	0	0	0	0	0
445	0	0	0	0	0
446	0	0	0	0	0
447	0	0	0	0	0
448	0	0	0	0	0
449	0	0	0	0	0
450	0	0	0	0	0
451	0	0	0	0	0
452	0	0	0	0	0
453	0	0	0	0	0
454	0	0	0	0	0
455	0	0	0	0	0
456	0	0	0	0	0
457	0	0	0	0	0
458	0	0	0	0	0
459	0	0	0	0	0
460	0	0	0	0	0
461	0	0	0	0	0
462	0	0	0	0	0
463	0	0	0	0	0
464	0	0	0	0	0
465	0	0	0	0	0

466	0	0	0	0	0
467	0	0	0	0	0
468	0	0	0	0	0
469	0	0	0	0	0
470	0	0	0	0	0
471	0	0	0	0	0
472	0	0	0	0	0
473	0	0	0	0	0
474	0	0	0	0	0
475	0	0	0	0	0
476	0	0	0	0	0
477	0	0	0	0	0
478	0	0	0	0	0
479	0	0	0	0	0
480	0	0	0	0	0
481	0	0	0	0	0
482	0	0	0	0	0
483	0	0	0	0	0
484	0	0	0	0	0
485	0	0	0	0	0
486	0	0	0	0	0
487	0	0	0	0	0
488	0	0	0	0	0
489	0	0	0	0	0
490	0	0	0	0	0
491	0	0	0	0	0
492	0	0	0	0	0
493	0	0	0	0	0
494	0	0	0	0	0
495	0	0	0	0	0
496	0	0	0	0	0
497	0	0	0	0	0
498	0	0	0	0	0
499	0	0	0	0	0
500	0	0	0	0	0

403

404 **File S2.** R routine to correct abundance when populations are partly in noise.

405

406 **R code**

407 The code below describes how to implement an R routine to correct the abundance of
 408 picoplanktonic populations based on their red fluorescence distribution. All libraries used here are
 409 freely available from R repositories. The input file used in this examples is named as Pro_C6.txt (See
 410 input file example File S1). This file has been created by exporting FL3 (chlorophyll) histogram from
 411 the Flowing Software (<http://www.flowingsoftware.com>) combining different samples into a single
 412 file. The first column contains the channel number and each following column corresponds to a
 413 different sample with rows corresponding to cell counts in each channel. Such a file could be created
 414 with any flow cytometry software. After running the `cyto_plot` function, a pdf output file is created
 415 named "Pro_C6.txt 1.0 .pdf" which contains all histograms from the input file (see File S3)and the file
 416 statistics (sample, uncorrected and corrected total cell abundance) are available as a data frame in the R
 417 session (see example at bottom of this file)

418

419

420 **# Example of use of cyto_plot function (run first the R code below to define the necessary functions)**421 `stats_Pro_C6<-cyto_plot("Pro_C6.txt", decades_C6, channel_min_C6, xmin_C6, xmax_C6)`

422

423 **# Example of statistics output**

424

425	<code>sample</code>	<code>cell_tot</code>	<code>cell_tot_correc</code>
426	1 sample135_C6_PRO_5m	134	cells in noise
427	2 sample136_C6_PRO_50m	111	cells in noise
428	3 sample137_C6_PRO_110m	13072	20240
429	4 sample138_C6_PRO_130m	3598	no correction
430	5 sample139_C6_PRO_170m	2211	no correction

431

432

433 **R code**434 **# Install libraries**

435 library("ggplot2")

436 library("reshape2")

437 library("plyr")

438 library("scales")

439 require(grid)

440

441 **# Set the working directory where the files are located**

442 setwd ("C:/My Documents/cytometry data/")

443

444 **# Define basic parameters**

445 decades_Canto = 5

446 decades_C6 = 7

447 channel_min_Canto = 100

448 channel_min_C6 = 214

449 xmin_Canto = 10

450 xmin_C6 = 1000

451 xmax_Canto = 10000

452 xmax_C6 = 100000

453 channel_max = 500

454 point <- format_format(big.mark = "", decimal.mark = ".", scientific = TRUE)

455 **# -----**456 **# cell_correct(channel, cell_number, cell_smooth)**457 **# Arguments**458 **# channel : vector containing the channels (from 1 to 500 in the present case)**459 **# cell_number : vector containing cell abundance in each channel**460 **# cell_smooth : vector containing smoothed cell abundance in each channel**461 **# Description**462 **# This function determines in which case we are ("no correction", "cells in noise" or "correction") and**463 **return the corrected cell abundance in the latter case.**

464

465 cell_correct<-function(channel, cell_number, cell_smooth)

466 { df<-data.frame(channel, cell_number, cell_smooth) **# create a data frame**467 i_min<-which.min(channel) **# determine the minimum channel**

```

468 i_max<-which.max(channel) # determine the maximum channel
469 i_cell_max<-which.max(cell_smooth) # determine in which channel is the histogram mode
470
471 # "no correction" : cell abundance in the first channel is 5 times lower than abundance at the maximum
472 of the histogram
473 if (cell_smooth[i_cell_max]>5*cell_smooth[i_min]) {cell_correct<-"no correction"}
474 # "cells in noise" : maximum of cell abundance is in the first channel
475 else {if (i_cell_max==i_min)
476       {cell_correct<-"cells in noise"}
477 # "correction" : all the other cases, we then apply a correction by computing the total cell abundance
478 as twice the number of cells in the channels right of the histogram maximum
479 else
480       {cell_correct<-2*sum(cell_number[i_cell_max:i_max])}
481     }
482 return (cell_correct)
483 }
484
485 # -----
486 #cyto_plot(file_name,decades,channel_min,xmin,xmax)
487 # Arguments
488 # file_name : name of input file containing the different samples (see File S1)
489 # decades : number of logarithmic decades of the flow cytometer (e.g. 7 for C6)
490 # channel_min : threshold channel for the histogram (depends on fcm acquisition settings)
491 # xmin : linear value corresponding to the threshold channel
492 # xmax : linear value corresponding to the maximum channel
493 # Description
494 # This function plots a set of histograms for the input samples,saves the graphics as a pdf file and
495 compute the total cell abundance indicating whether a corrections is needed or not. It returns a
496 dataframe containing three columns : sample, cell_tot, cell_tot_correc (see top of this file for an
497 example)
498
499 cyto_plot<-function(file_name,decades,channel_min,xmin,xmax)
500 {
501   channel_max = 500 # this the number of channels provided as output of the Flowing Software
502   histo<- read.delim(file_name)
503   histo<- histo[histo$channel>=channel_min,]
504   histo_melt<- melt(histo, id.vars=c("channel"),variable.name = "sample", value.name =

```

```

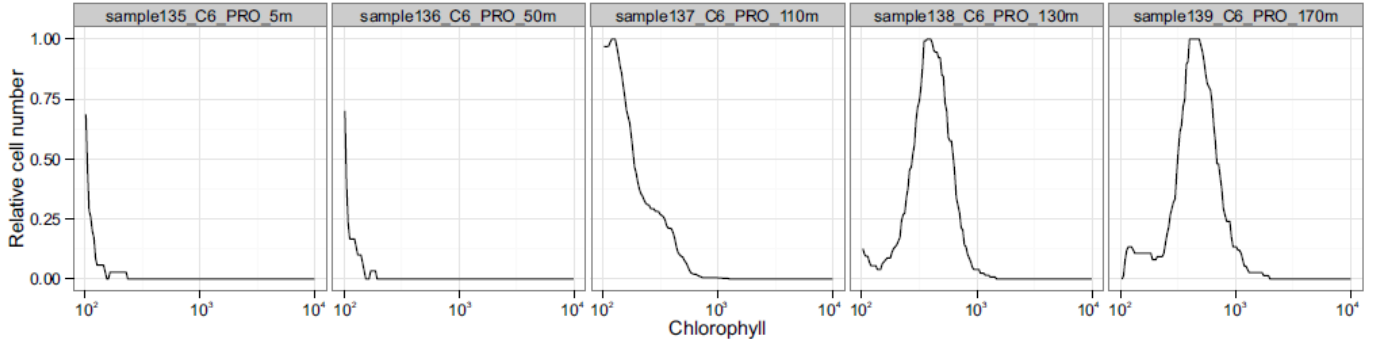
505
506
507 # smooth histogram using default R smoothing function
508     histo_melt<- ddply(histo_melt,c("sample"), transform,
509 cell_smooth=as.vector(smooth(cell_number)))
510 # normalize histogram so that maximum abundance is equal to 1
511     histo_melt<- ddply(histo_melt,c("sample"), transform, cell_norm=cell_smooth/max(cell_smooth))
512 # transform log channel to linear scale for plotting
513     if (decades==5)
514         {histo_melt<- ddply(histo_melt,c("sample"), transform,
515 fluo=(10^5)^(channel/channel_max))}
516     else
517         {histo_melt<- ddply(histo_melt,c("sample"), transform,
518 fluo=(10^7)^(channel/channel_max))}
519 # plots histograms using 5 columns
520     histo_plot<-ggplot(histo_melt, aes(fluo,cell_norm)) + geom_line() + theme_bw () + facet_wrap(~
521 sample, nrow=21, ncol=5) + xlab("Chlorophyll")+ylab("Relative cell number") +
522 scale_x_log10(limits=c(xmin,xmax), labels=point)
523 # save plots as pdf
524 ggsave(plot=histo_plot, filename=paste(file_name," 1.0 .pdf",sep=""),width = 15, height = 4, scale=2,
525 units="cm")
526 # compute uncorrected and corrected total cell number calling the cell_correct function defined above
527     stats<-ddply(histo_melt,c("sample"), summarise,
528 cell_tot=sum(cell_number),cell_tot_correc=cell_correct(channel,cell_number,cell_smooth))
529     print(paste("# of decades:",decades,"minimum channel : ",channel_min, "xmin : ", xmin, " xmax
530 : ", xmax))
531     print (paste("File : ",file_name))
532     stats
533     return (stats)
534 }
535
536
537
538

```

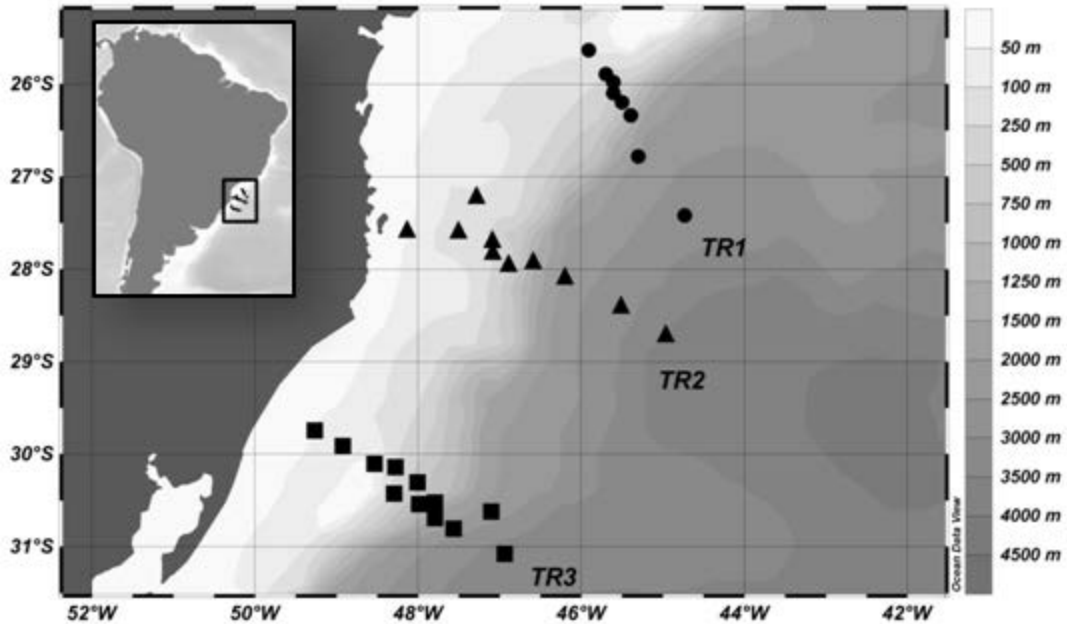
539

540 **File S3.** Example of output file for R routine.

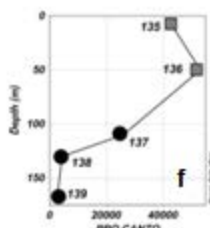
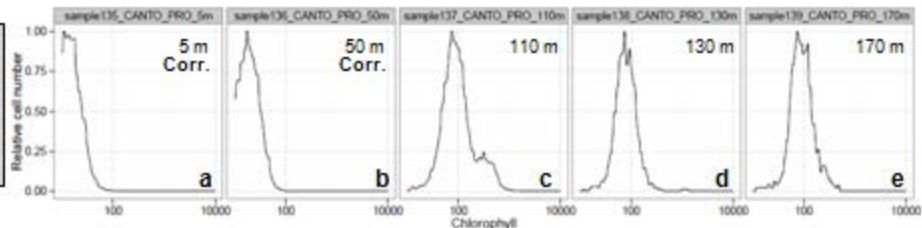
541



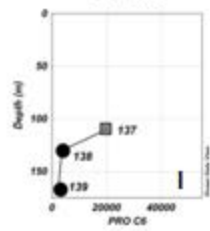
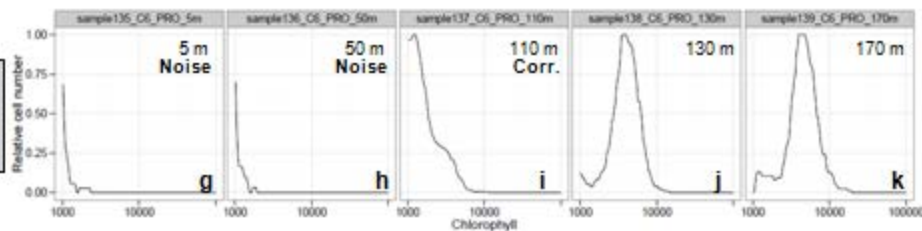
542



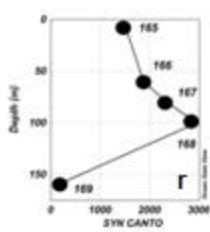
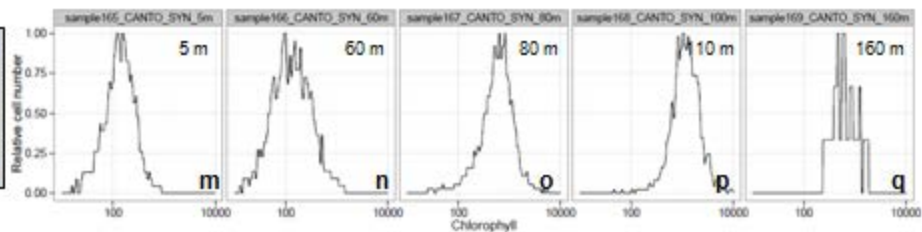
PRO - CANTO



PRO - C6



SYN - CANTO



SYN - C6

